Original Paper

International Archives of Allergy and Immunology

Int Arch Allergy Immunol 2012;159:367–383
DOI: 10.1159/000338288

Received: October 1, 2011
Accepted after revision: March 14, 2012
Published online: July 26, 2012

Allergic Airway Inflammation in Mice Deficient for the Antigen-Processing Protease Cathepsin E

Carolin Pilzner[a, c] Frank Bühling[d] Thomas Reinheckel[e] Caroline Chwieralski[f] Anchana Rathinasamy[b] Hans-Dieter Lauenstein[a, c] Thomas Wex[g] Tobias Welte[a] Armin Braun[c] David A. Groneberg[a, h, i]

Departments of [a]Pneumology and [b]Immunology, Hannover Medical School, and [c]Department of Airway Immunology, Fraunhofer Institute for Toxicology and Experimental Medicine ITEM, Hannover, [d]Institute of Laboratory Medicine, Carl-Thiem-Klinikum, Cottbus, [e]Institute of Molecular Medicine and Cell Research, Albert Ludwigs University of Freiburg, Freiburg, [f]Institute of Immunology and [g]Clinic of Gastroenterology, Hepatology and Infectious Diseases, Otto-von-Gruericke University Magdeburg, Magdeburg, [h]Institute of Occupational Medicine, Charité – Universitätsmedizin Berlin, Berlin, and [i]Department of Pneumology, Institute of Occupational Medicine, Social Medicine and Environmental Medicine, Goethe University Frankfurt Frankfurt/Main, Germany

Key Words
Dendritic cell · Airway inflammation · Cathepsin E

Abstract
Background: Allergic asthma is a Th2-type chronic inflammatory disease of the lung. It is characterized by infiltration of eosinophils, neutrophils, mast cells and T lymphocytes into the airways. Th2 cytokines like interleukin (IL)-4, IL-5 and chemokines like eotaxin are increased in the asthmatic response. The processing and presentation of exogenous antigens is important in the sensitization to an allergen. Cathepsin E (Ctse) is an intracellular aspartic endoprotease which is expressed in immune cells like dendritic cells (DCs). It was found to play an essential role in the processing and presentation of ovalbumin (OVA). The aim of the present study was to investigate the inhibition of Ctse in two different experimental models of allergic airway inflammation. ***Methods:*** Ctse wild-type ($Ctse^{+/+}$) and Ctse-deficient ($Ctse^{-/-}$) bone marrow-derived DCs (BMDCs) were pulsed with OVA/OVA peptide and cocultured with OVA transgenic T II (OT II) cells whose proliferation was subsequently analyzed. Two different in vivo asthma models with $Ctse^{+/+}$ and $Ctse^{-/-}$ mice were performed: an acute OVA-induced and a subchronic *Phleum pratense*-induced airway inflammation. ***Results:*** Proliferation of OT II cells was decreased when cocultured with BMDCs of $Ctse^{-/-}$ mice as compared to cells cocultured with BMDCs of $Ctse^{+/+}$ mice. In vivo, Ctse deficiency led to reduced lymphocyte influx after allergen sensitization and challenge in both investigated airway inflammation models, compared to their control groups. ***Conclusion:*** Ctse deficiency leads to a reduced antigen presentation in vitro. This is followed by a distinct effect on lymphocyte influx in states of allergic airway inflammation in vivo.

Copyright © 2012 S. Karger AG, Basel

Introduction

Cathepsin E (Ctse) is an intracellular aspartic protease of the pepsin superfamily that exists as a disulfide-linked homodimer with a molecular mass of approximately 90

KARGER

Fax +41 61 306 12 34
E-Mail karger@karger.ch
www.karger.com

© 2012 S. Karger AG, Basel
1018–2438/12/1594–0367$38.00/0

Accessible online at:
www.karger.com/iaa

Correspondence to: Prof. David Groneberg
Department of Pneumology, Institute of Occupational Medicine
Social Medicine and Environmental Medicine, Goethe University Frankfurt
Theodor-Stern-Kai 7, DE–60590 Frankfurt/Main (Germany)
Tel. +49 69 6301 6650, E-Mail groneberg@med.uni-frankfurt.de

kDa and as a monomer of 43 kDa [1]. It is highly homologous to the analogous aspartic protease cathepsin D [2]. Ctse is mainly present in cells of the immune system, including antigen-presenting cells (APCs) such as dendritic cells (DCs), macrophages (Mph) [3], lymphocytes [4], and is also present in microglia [5], Langerhans cells and interdigitating reticulum cells [6]. It has also been detected in gastric [1] and lung epithelial cells [7]. Depending on the species and cell type, Ctse has been reported to be localized in different cellular compartments, such as plasma membranes [8], endosomal structures [5, 9], the endoplasmic reticulum and the Golgi apparatus [5, 10, 11]. Studies with Ctse-deficient mice ($Ctse^{-/-}$) have shown that they do not exhibit any phenotypic alterations when reared under specific pathogen-free conditions [4]. These mice were fertile and showed normal breeding behavior. Kept under non-pathogen-free conditions, these mice developed atopic dermatitis-like skin lesions [12] and showed increased susceptibility to bacterial infections [13]. Ctse has been suggested to play a role in antigen processing via the major histocompatibility complex class II (MHC II) [2]. The involvement of Ctse in antigen processing was first shown by Bennett et al. [14] in 1992. A Ctse-specific inhibitor of *Ascaris lumbricoides* was used in this study, and the authors were able to demonstrate that Ctse is essential for ovalbumin (OVA) processing by murine B cells. Related results were achieved using cathepsin D-deficient mice to study the role of Ctse in antigen presentation by microglia [15] and DCs by additional blocking of Ctse with a new synthesized inhibitor called MPC6 [3].

DCs are bone marrow-derived migratory cells that are present in most tissues, including the gut [16] and the lung [17]. Their major role is to sample environmental antigens (Ag) and to present antigenic peptides in the local lymph node [18]. In APCs, two distinct proteolytic events are required to trigger the MHC II pathway, the processing of the invariant chain and the processing of antigen substrates [19, 20].

Recent evidence indicates that aspartic proteases such as cathepsin D and Ctse are required for both invariant chain and Ag processing [20–23]. Ctse was found to play an essential role in the processing and presentation of the full OVA protein but not of OVA-derived peptides. Moreover, in DCs, Ctse is present in the early endosomes and is involved in the processing of exogenous antigens [2]. This processing and the presentation of exogenous antigens are important in the sensitization to an allergen. This allergen can activate DCs to break the process of tolerance and promote Th2 responses such as allergic asthma [24].

Allergic asthma is a chronic type-2 Th2 inflammatory disease of the airways affecting approximately 300 million individuals worldwide [25]. Over the past 30 years, the prevalence of asthma has increased dramatically in many Western countries and is now greater than 10% [26]. Allergic asthma is induced by the sensitization to an allergen. This process begins with the uptake of an antigen by airway DCs [27]. These DCs migrate to draining mediastinal lymph nodes to prime naive T cells [28, 29]. These allergen-specific T cells enter the airways where they reside, even during asymptomatic periods [30, 31]. Reexposure to the antigen triggers a Th2-driven allergic inflammation characterized by the release of Th2-associated cytokines, such as interleukin (IL)-4 and IL-5, recruitment of eosinophils, mucus hypersecretion, smooth muscle cell hyperreactivity and airway remodeling [32]. As reported, lung DCs are required for the development of the Th2 phenotype of allergic asthma and their essential role in this disease has been shown [29].

In view of the reported involvement of Ctse in the processing and presentation of exogenous Ag in DCs, which are essential for the initiation and maintenance of allergic asthma, we hypothesized that an inhibition of Ctse would lead to a decrease in allergic airway inflammation because of decreased antigen processing and presentation of the allergen. In the present study, we evaluated the effect of Ctse deficiency in a model with acute OVA-induced airway inflammation and in another model with subchronic airway inflammation induced by grass pollen (*Phleum pratense* extract).

Materials and Methods

Mice

$Ctse^{-/-}$ mice (6–8 weeks old) were generated by the authors by gene targeting in HM1 embryonic stem cells. Before the study commenced, all mice had been backcrossed onto the C57BL/6N genetic background for 10 generations and maintained under specific pathogen-free conditions. All animals were kept in a regular 12-hour light/dark cycle with food and water ad libitum. The animal experiments reported here were conducted in compliance with the German Animal Welfare Law and with the European Communities Council Directive 86/609/EEC for the protection of animals used for experimental purposes. All experiments were performed according to a reviewed protocol approved by the Animal Ethics Committee (permit No. 06/1177 and 08/1610; competent authority 'Niedersächsisches Landesamt für Verbraucherschutz und Lebensmittelsicherheit').

In vitro Antigen Presentation

Bone marrow-derived dendritic cell (BMDC) generation was performed according to a protocol adapted from Lutz et al. [33].

Briefly, bone marrow cells were rinsed out of femur and tibia of Ctse wild-type ($Ctse^{+/+}$) and Ctse-deficient ($Ctse^{-/-}$) mice and resuspended in RPMI 1640 (with 1% penicillin-streptomycin, 10% fetal calf serum and 2 mM β-mercaptoethanol (all from Sigma, Taufkirchen, Germany)). 30×10^6 cells were seeded into a tissue culture flask with granulocyte Mph colony-stimulating factor (final concentration 20 ng/ml; Sigma), and were cultured for 9 days. On day 8 BMDCs were transferred to a 24-well cell culture plate. The BMDCs were stimulated with or without 5 μg lipopolysaccharide (LPS; Sigma) for 24 h and were pulsed with either 50 μg OVA peptide or with different concentrations of OVA (1, 0.5, 0.1 mg/ml; both from Sigma). On day 9 the BMDCs were cocultured with OVA-transgenic T cells (OT II cells). On day 11 the cocultured cells were marked with ^{3}H-thymidine and on day 12 proliferation of the OT II cells was analyzed.

Acute Model of Allergic Airway Inflammation Induced by Intraperitoneal Sensitization

$Ctse^{+/+}$ and $Ctse^{-/-}$ mice were sensitized as described previously [34]. Briefly, mice were sensitized intraperitoneally with 10 μg OVA (grade VI; Sigma) combined with 1.5 mg aluminum hydroxide (alum; $Al(OH)_3$; Imject Alum, Pierce, Rockford, Ill., USA) in 200 μl saline on days 0, 14 and 21. Animals in the control group received saline combined with alum instead. On days 27 and 28 the animals were exposed to 1% OVA aerosol for 20 min. Twenty-four hours later they were sacrificed by injection of an overdose of pentobarbital sodium. Bronchoalveolar lavage (BAL) was performed by rinsing twice with 0.8 ml phosphate-buffered saline (PBS).

Chronic Model of Airway Inflammation Induced by Airway Sensitization

$Ctse^{+/+}$ and $Ctse^{-/-}$ mice were sensitized as described previously [35]. Briefly, animals were sensitized intranasally with *P. pratense* extract (9 μg major allergen in 50 μl sodium chloride; ALK Abelló, Horsholm, Denmark) on 2 consecutive days per week over a period of 11 weeks. Control mice received sodium chloride (NaCl). On day 72 the mice were sacrificed by injection of an overdose of pentobarbital sodium. Blood was collected via the vena cava and BAL was performed by rinsing twice with 0.8 ml PBS. Lungs were filled with diluted OCT kryotek (1:3 in PBS; Sakura Finetek, Staufen, Germany) and frozen in liquid nitrogen for the preparation of lung cryosections.

Plasma Sampling

Mice were bled via the vena cava. Heparin plasma was prepared by centrifugation at 150.000 *g* for 10 min and preserved at –20°C for determination of *P. pratense*-specific IgG and IgE.

Bronchoalveolar Lavage

BAL was performed by flushing twice with 800 μl PBS. BAL fluid was centrifuged and supernatants were stored at –20°C for cytokine measurement. Cells were resuspended and counts were determined electronically (CASY, Schärfe Systems, Germany). To this end 0.5×10^6/ml cells were loaded on a cytospin and stained according to Pappenheim and a differential cell count of 300 cells per slide was performed.

Lung Histology

After BAL lungs were filled with OCT (1:3 in PBS) and snap-frozen in liquid nitrogen. Cryosections (14 μm) were obtained and stained according to Azan novum. Cryosections were stained with nuclear fast red aluminum sulfate solution (Merck, Darmstadt, Germany) for 40 min, washed twice with aqua bidest and incubated with 5% phosphotungstic acid hydrate (Merck) for 10 min. After two washing steps with aqua bidest, the cryosections were stained with a mixture of aniline blue and orange G (both from Sigma, Munich, Germany) for 1 min and 20 s. Cryosections were washed twice with aqua bidest, incubated with isopropanol and fixed with xylene (both from Roth, Karlsruhe, Germany).

Cytokine Measurement

IL-4, IL-5, IL-13, IFN-γ and eotaxin-1 (CCL11) concentrations were determined in duplicates by enzyme-linked immunosorbent assay (ELISA; Duoset, R&D Biosciences, Wiesbaden-Nordenstadt, Germany) in pg/ml according to the instructions given in the user manual. The lower limits of quantification were 15.6 pg/ml for IL-4, 31.3 pg/ml for IL-5, 62.5 pg/ml for IL-13, 31.3 pg/ml for IFN-χ and 7.8 pg/ml for eotaxin-1.

P. pratense-*Specific IgG and IgE in Plasma*

P. pratense-specific plasma IgG and IgE concentrations were determined by ELISA. A 96-well plate was coated overnight with 1 μg recombinant *P. pratense* (Biomay, Vienna, Austria). On the next day the plate was washed five times with wash buffer (PBS with 0.1% Tween). After blocking and incubation of the samples, the 96-well plate was coated with either 0.2 μg/ml of the horseradish peroxidase (HRP)-conjugated IgG antibody (Abbiotec, Cologne, Germany) or 2 μg/ml of the HRP-conjugated IgE antibody (Serotec, Düsseldorf, Germany) to measure the amounts of *P. pratense*-specific IgG and IgE.

In vivo Antigen Processing with DQ™ OVA

$Ctse^{+/+}$ and $Ctse^{-/-}$ mice received 50 μg DQ™ OVA (Invitrogen, Karlsruhe, Germany) and 0.1 μg LPS (Sigma, Taufkirchen) intranasally on 3 consecutive days under isoflurane anesthesia. Control mice were untreated. DQ™ OVA is a self-quenched conjugate of OVA that exhibits bright green fluorescence upon proteolytic degradation. On day 4 mice were sacrificed by pentobarbital sodium injection. Lung tissue was resected, disrupted and digested with 2 mg/ml collagenase type III (Worthington Biochemical Corp., Lakewood, N.J., USA) and 0.1% DNase I (Roche Diagnostics, Mannheim, Germany) during a 30-min incubation period at 37°C. The digested tissue was homogenized and filtered through a steel sieve with pore size of 100 μm. After lysis of erythrocytes, $CD11c^+$ cells were isolated by magnetic cell sorting (Miltenyi Biotec, Bergisch Gladbach, Germany). The $CD11c^+$-enriched cells were stained with allophycocyanin (APC) monoclonal antibody (mAb) to CD11c and phycoerythrin (PE) monoclonal antibody to MHC class II or the appropriate isotype controls (all from BD Biosciences, Heidelberg, Germany) and used for fluorescence-activating cell sorting (FACS; FACSaria, BD Biosciences). DCs were identified and defined as $CD11c^+$ MHC II^{high} cells, whereas tissue Mph were defined as $CD11c^+$MHC II^{low} phenotype.

In vivo Antigen Presentation with OT II Cells

OT II cells were isolated from lymph nodes and spleens of OT II-transgenic mice. After determination of the number and viability of the cells, spleen and lymph node cells were stained with

Table 1. Primer sequences of the analyzed cathepsins and the housekeeping gene PBGD

Gene		Sequence	Product size
Cathepsin B	Sense	5′-agg gtt gcg ttc ggt gag-3′	350 bp
	Anti-sense	5′-cag gga atg gtg tat gg-3′	
Cathepsin C	Sense	5′-gag aaa atg agc ctg cga ga-3′	374 bp
	Anti-sense	5′-tct tcc acc acc cca aaa-3′	
Cathepsin D	Sense	5′-gtc gtc ttt gat act ggc tcc t-3′	270 bp
	Anti-sense	5′-ctg ctt ggt ggc ttc tcc-3′	
Cathepsin E	Sense	5′-cag tcc gac aca tac acg-3′	154 bp
	Anti-sense	5′-tgg cct ggc tcc ttg ac-3′	
Cathepsin H	Sense	5′-aag att caa gcc cac aac ca-3′	307 bp
	Anti-sense	5′-cag cca aag aca gca ttt tc-3′	
Cathepsin K	Sense	5′-gct tgg cat ctt tcc agt ttt-3′	200 bp
	Anti-sense	5′-gca ggc gtt gtt ctt att cc-3′	
Cathepsin L	Sense	5′-ctt ttg gct gct ctc tgc tt-3′	297 bp
	Anti-sense	5′-cct ccc ctt ctt gtg ctt c-3′	
Cathepsin S	Sense	5′-act gtg gac tgg aga gag aag g-3′	370 bp
	Anti-sense	5′-ctt tca ggg cat cct cgt-3′	
PBGD	Sense	5′-atc cag gtc cct gtt cag caa gaa-3′	181 bp
	Anti-sense	5′-cat taa gct gcc gtg caa cat cca-3′	

carboxyfluorescein succinimidyl ester (CFSE) and injected intravenously into $Ctse^{+/+}$ and $Ctse^{-/-}$ mice. On the next day the $Ctse^{+/+}$ and $Ctse^{-/-}$ mice were challenged with 1% OVA aerosol for 1 h (sensitized mice) or with NaCl aerosol (control mice). Four days later, the $Ctse^{+/+}$ and $Ctse^{-/-}$ mice were sacrificed by injection of an overdose of pentobarbital sodium. Lung-draining lymph nodes were removed, mashed on a gossamer and stained with antibodies specific for the surface markers CD4, Ly5.1, CD44, CD25 and anti-TCR-Vβ5.1 bio (biotin) OT II for OVA transgenic T cell receptor (Invitrogen; BD Bioscience) or the appropriate isotype controls (all from BD Bioscience). The CFSE profile was assessed for TCR-Vβ5.1 OT II-positive cells by flow cytometry (LSRII, BD Bioscience).

Generation of BMDCs

BMDC generation was performed according to a protocol adapted from Lutz et al. [33]. Briefly, bone marrow cells were rinsed out of femur and tibia of naive C57/BL6N mice and, following red blood cell lysis, resuspended in tissue culture medium consisting of RPMI-Glutamax (Gibco, Invitrogen) with 1% penicillin-streptomycin (Lonza, Verviers, Belgium), 5% fetal calf serum, 50 μM β-mercaptoethanol and granulocyte Mph colony-stimulating factor (final concentration 20 ng/ml; both from Sigma, Taufkirchen). 5×10^5 cells/well were seeded into 6-well tissue culture plates and cultured for 10 days. The in vitro-generated BMDCs were stored directly in RLT buffer for real-time PCR or in lysis buffer for Western blot analysis.

Lung DC Isolation

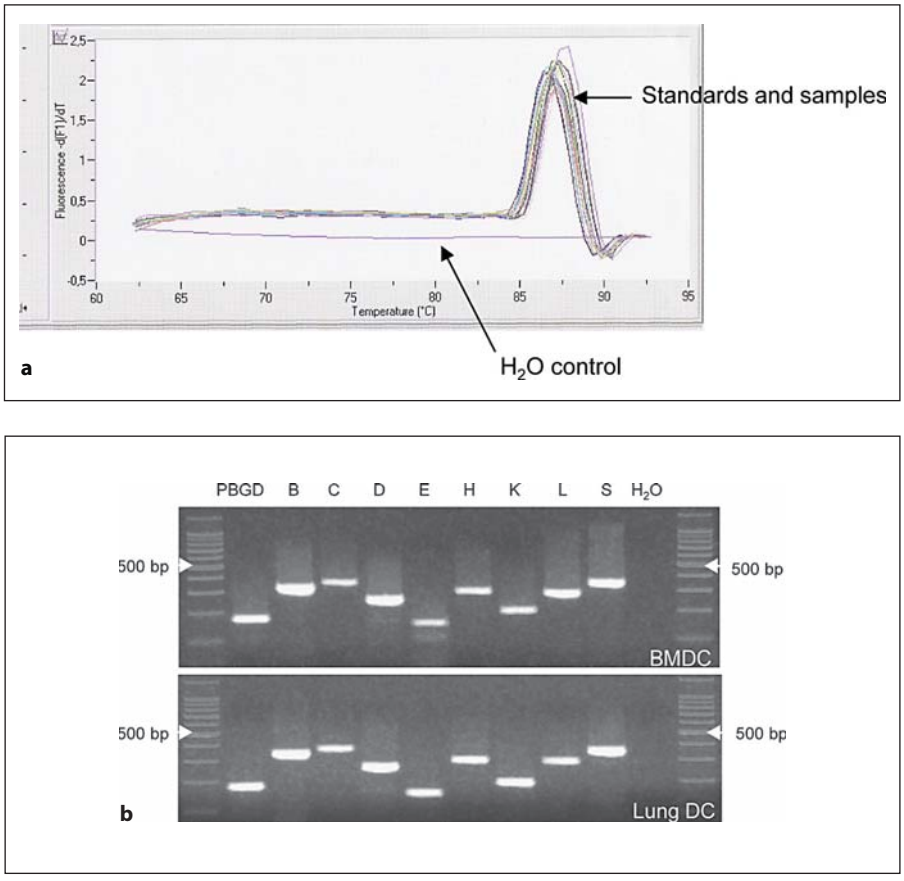
Lung tissue was resected, disrupted and digested with 2 mg/ml collagenase type III (Worthington Biochemical Corp.) and 0.1% DNase I (Roche Diagnostics) during a 30-min incubation period at 37°C in a shaking water bath. The digested tissue was homogenized and filtered through a steel sieve with a pore size of 100 μm. After lysis of erythrocytes, $CD11c^+$ cells were isolated by magnetic separation (Miltenyi Biotec). The $CD11c^+$-enriched cells were stained with allophycocyanin (APC) labeled antibody to CD11c and PE-labeled antibody to MHC class II or the appropriate isotype controls (all from BD Biosciences) and used for FACS (FACSaria, BD Biosciences). DCs were identified and defined as $CD11c^+$ MHC II^{high} cells, whereas contaminating tissue Mph were defined as MHC II^{low} phenotype. The sorted DCs were stored directly in RLT buffer for real-time PCR or in lysis buffer for Western blot analysis.

Cell Surface Markers on BMDCs and Lung DCs

Before using the in vitro-generated BMDCs and isolated lung DCs for PCR experiments, cells were stained for different cell surface markers such as PE-labeled MHC II, allophycocyanin (APC) labeled CD11c, fluorescein isothiocyanate (FITC)-labeled CD86 and CD40 (all from BD Biosciences) and FITC-labeled CD80 (AbD Serotec, Oxford, UK) or the appropriate isotype controls (BD Biosciences; AbD Serotec) and were analyzed by flow cytometry (FACSaria, BD Biosciences).

Real-Time PCR and Quantification

From in vitro-generated BMDCs and isolated lung DCs of naive C57BL/6 mice, RNA was extracted using RNeasy Plus kit and reverse transcribed with Omniscript RT kit or Sensiscript RT kit (all from Qiagen, Hilden, Germany). cDNA was analyzed for the expression of cathepsins B, C, D, E, H, K, L and S by real-time PCR and was normalized to the housekeeping gene porphobilinogen deaminase (PBGD; table 1 shows primer sequences of the analyzed cathepsins and the housekeeping gene PBGD).



Color version available online

Fig. 1. Real-time PCR analysis of in vitro-generated BMDCs and isolated lung DCs. cDNA of in vitro-generated BMDCs and isolated lung DCs was analyzed for the expression of cathepsins B, C, D, E, H, K, L and S and the housekeeping gene PBGD by real-time PCR. Target gene expression was quantified using Light Cycler Fast Start DNA Master SYBR Green. For quantification, plasmids of the appropriate cathepsins were used as standards. **a** Melting curves of standards and samples of PBGD in BMDCs and lung DCs. **b** Gel electrophoresis of cDNA of PBGD, cathepsin B, C, D, E, H, K, L and S.

All primers were designed to be intron-spanning to avoid contamination of genomic DNA. PCR products were verified via melting curves and gel electrophoresis (fig. 1a, b). Target gene expression was quantified using Light Cycler Fast Start DNA Master SYBR Green (Roche Diagnostics). For quantification, plasmids of the appropriate cathepsins were used as standards. These plasmids were prepared according to the data sheet instructions of the PCR Purification Kit, the Cloning^{plus} Kit and the Plasmid DNA Purification Kit (all from Qiagen). After determination of the DNA content of the generated plasmid standards by measuring the extinction of 260 nm by photometer, the DNA concentration of all standards was set to 1 μg/ml and then diluted up to 10^{-10}. After expression analysis of the different cathepsins in BMDCs and lung DCs by real-time PCR, the DNA content and the resulting transcript numbers were determined using the following formula and were normalized to the housekeeping gene PBGD:

$$[(\text{DNA})\ \text{g/l}: MW_{DNA}\ \text{g/l}] \times 6 \times 10^{23} = \text{transcripts mol/l}$$
$$MW_{DNA} = 660\ \text{g/mol} \times \text{number bp}$$

Western Blot Analysis

Isolated lung DCs and in vitro-generated BMDCs were disrupted in lysis buffer (50 mM sodium acetate, 1 mM EDTA, 0.05% Brij, pH 5.5) by Dounce homogenization (Wheaton, Millville, N.J., USA). A postnuclear supernatant was produced by centrifugation at 1,500 *g* for 10 min. Subsequently 50 μg of protein from the postnuclear supernatant were resolved by 15% SDS-PAGE and transferred onto polyvinylidene difluoride (PVDF) membranes. Primary antibodies for immunodetection of cathepsins on the PVDF membranes were goat anti-cathepsin B, anti-cathepsin L and anti-cathepsin S (all from R&D Systems, Wiesbaden, Germany; 1:500 dilution) and secondary antibody anti-goat HRP (Sigma, Hamburg, Germany; 1:5,000 dilution). For loading control α-tubulin was detected by monoclonal antibodies (Sigma, Munich; 1:1,000 dilution) in combination with goat anti-mouse IgG (Calbiochem/Merck, Darmstadt, Germany; 1:1,000 dilution) as secondary antibody. Detection of the peroxidase-labeled secondary antibodies was performed by enhanced chemiluminescence reaction (Thermo Scientific, Rockford, Ill., USA) and visualization using the Lumi-Imager system and Lumi-Analyst software (Roche Diagnostics).

Statistical Analysis

Data are displayed as means ± standard error of the mean (SEM) for the indicated number of experiments. To detect significant differences between groups statistical analyses using the t test or analyses of variance (ANOVA) with Bonferroni's multiple comparison test were performed (GraphPad Prism® software, version 4.03). p values <0.05 were considered to be significant.

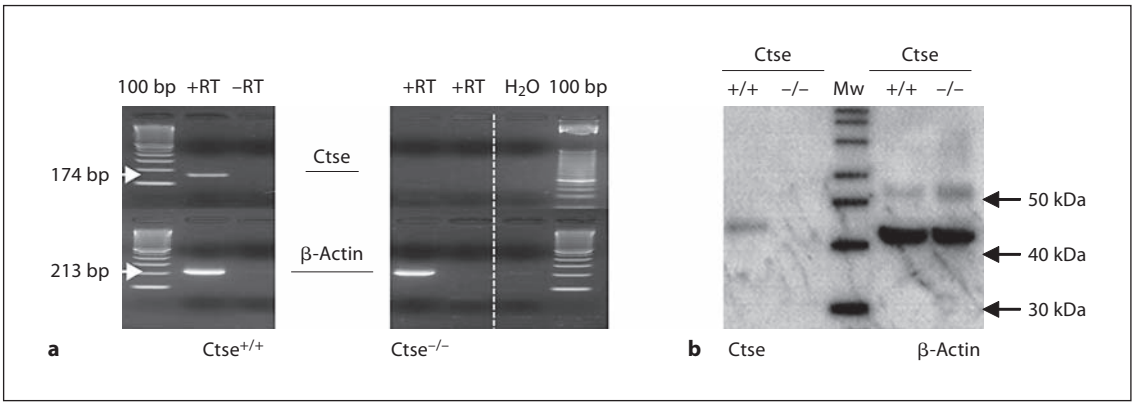


Fig. 2. Expression of cathepsin E in lung and spleen of Ctse$^{+/+}$ and Ctse$^{-/-}$ mice. **a** Representative image of PCR products from reverse-transcribed RNA isolated from lungs of Ctse$^{+/+}$ and Ctse$^{-/-}$. Ctse was detected by the primer pair 5′-CAG TCC GAC ACA TAC ACG-3′/5′-GG CCT GGC TCC TTG AC-3′ and the positive control β-actin by the primer pair 5′-ACC CAG GCA TTG CTG ACA GG-3′/5′-GGA CAG TGA GGC CAG GAT GG-3′. Cycling conditions: 95°C for 15 s, 60°C for 30 s, 72°C for 30 s for 50 cycles. **b** Western blot analysis of Ctse in spleens of Ctse$^{+/+}$ and Ctse$^{-/-}$ mice; loading control β-actin. Mw = Molecular weight marker; +RT/–RT = with reverse transcription (cDNA)/without reverse transcription (RNA).

Results

Expression of Cathepsin E in Lung and Spleen of Ctse$^{+/+}$ and Ctse$^{-/-}$ Mice

The strain of Ctse$^{-/-}$ mice used in the present study had recently been generated by the authors and backcrossed for 10 generations to the C57BL/6N genetic background. Ctse$^{-/-}$ mice are viable and fertile with no gross phenotypes. RT-PCR analysis of mRNA samples from the lungs of mice confirmed the absence of Ctse expression in the Ctse$^{-/-}$ mice (fig. 2a). Their spleen contains large numbers of immune cells that are known to produce high amounts of Ctse. Western blot analysis of spleens from Ctse$^{+/+}$ and Ctse$^{-/-}$ mice confirmed the absence of the protease in the gene-targeted animals on the protein level (fig. 2b).

Reduced Proliferation of OT II Cells Cocultured with BMDCs of Ctse$^{-/-}$ Mice

To investigate whether Ctse deficiency has an effect on antigen presentation, we generated BMDCs of Ctse$^{+/+}$ and Ctse$^{-/-}$ mice. BMDCs were stimulated with or without LPS in combination with OVA peptide or different concentrations of OVA. OT II cells incubated with BMDC of Ctse$^{-/-}$ mice showed a significantly diminished proliferation compared to OT II cells cocultured with BMDCs of Ctse$^{+/+}$ mice. The reduced proliferation of OT II cells was shown by stimulation with OVA peptide as well as with different concentrations of OVA with LPS. Without LPS there was also a significant reduction in the proliferation of OT II cells incubated with BMDCs of Ctse$^{-/-}$ mice and stimulated with OVA, but there was no diminished proliferation when cells were stimulated with OVA peptide (fig. 3a, b). Consequently, Ctse deficiency impaired BMDC-mediated antigen presentation of OVA in vitro.

Ctse Deficiency Leads to Reduced Lymphocyte Influx after OVA Sensitization and Challenge

Based on the impaired presentation of OVA by Ctse$^{-/-}$ DCs in vitro we hypothesized that Ctse deficiency in DCs might lead to a reduced development and progression of acute OVA-induced allergic airway inflammation in vivo. As shown in figure 4a, the Ctse deficiency in Ctse$^{-/-}$ mice resulted in an inhibition allergen-induced infiltration of T lymphocytes ($p = 0.06$) into the lung, whereas in the sensitized Ctse$^{+/+}$ group lymphocyte numbers were increased. OVA sensitization and challenge resulted in a significant increase in eosinophils in both sensitized Ctse$^{+/+}$ and Ctse$^{-/-}$ groups compared to their respective control groups, without showing a difference in eosinophilic infiltration between Ctse$^{+/+}$ and Ctse$^{-/-}$ mice. Mph cell counts were not affected by the administration of OVA. In both positive groups, increased cell counts of neutrophil granulocytes were present (fig. 4a). As shown in figure 4b, the cytokine IL-5 increased significantly in

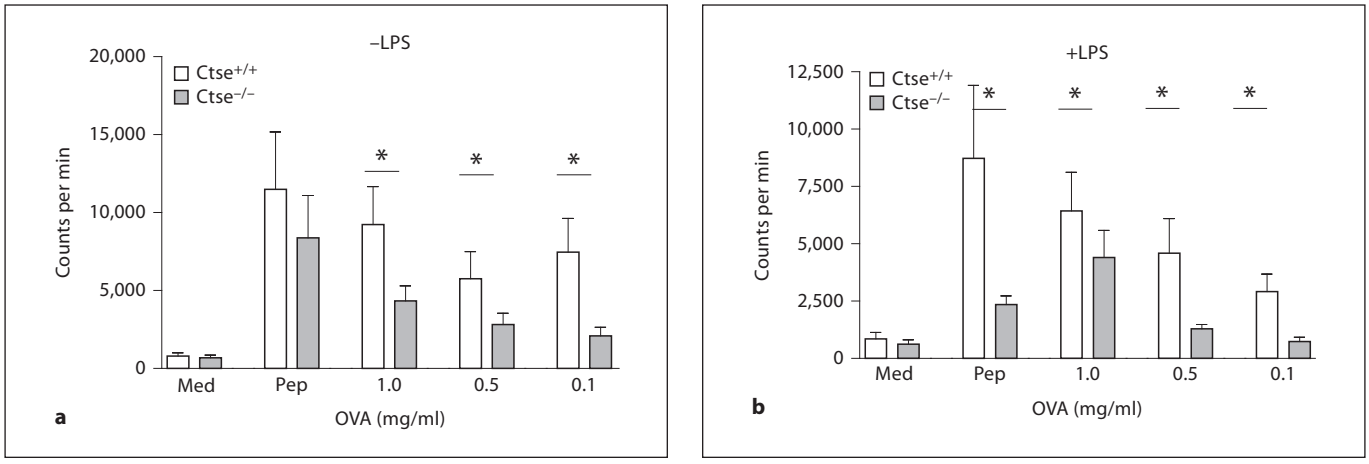


Fig. 3. Reduced proliferation of OT II cells cocultured with BMDCs of Ctse$^{-/-}$ mice. BMDCs of Ctse$^{+/+}$ (white bars) and Ctse$^{-/-}$ mice (grey bars) were stimulated with medium (Med), OVA peptide (Pep) or different concentrations of OVA (1, 0.5 and 0.1 mg/ml) without (**a**) or with (**b**) LPS and were cocultured with OT II cells. T cell proliferation was analyzed via the thymidine assay. Bars represent mean ± SEM of n = 3.

Table 2. Cytokines and chemokines in BAL fluid from Ctse$^{+/+}$ and Ctse$^{-/-}$ mice in the subchronic model of allergic airway inflammation

Cytokine/chemokine (pg/ml)	Ctse$^{+/+}$ ctrl (n = 12)	Ctse$^{+/+}$ sens (n = 6)	Ctse$^{-/-}$ ctrl (n = 12)	Ctse$^{-/-}$ sens (n = 12)
IL-4	60.58 ± 3.27	35.72 ± 2.07*	55.96 ± 6.23	39.19 ± 4.96
IL-5	72.12 ± 9.72	66.17 ± 13.88	56.72 ± 5.19	52.11 ± 8.02
IL-13	b.d.	b.d.	b.d.	b.d.
Eotaxin	73.73 ± 6.62	51.23 ± 3.75	42.25 ± 5.7	52.88 ± 4.34

Cytokine/chemokine levels in pg/ml in BAL fluid were measured using ELISA. * $p < 0.05$ in the t test. b.d. = Below detection limit; sens = mice sensitized with *P. pratense* extract; ctrl = control mice receiving saline.

Ctse$^{+/+}$ and Ctse$^{-/-}$ OVA groups without showing a difference between Ctse$^{+/+}$ and Ctse$^{-/-}$ mice, the chemokine eotaxin was not affected by administration of OVA, and the cytokines IL-4 and IFN-χ were below detection limit.

Reduced Lymphocyte Infiltration in Ctse$^{-/-}$ Mice after P. pratense *Sensitization*

To further address the question of whether Ctse deficiency plays a role in a sensitization via the airways, Ctse$^{+/+}$ and Ctse$^{-/-}$ mice were sensitized intranasally with *P. pratense* extract over a period of 11 weeks. As in the OVA-induced airway inflammation model, the sensitized Ctse$^{-/-}$ group showed inhibited lymphocyte infiltration, but this was not significant (fig. 5a). The airway sensitization resulted in a significant increase in eosinophils in both positive groups, but there was no difference in eosinophilic infiltration between Ctse$^{+/+}$ and Ctse$^{-/-}$ mice after sensitization. In addition, Mph cell counts were increased, but this effect was significant only in the Ctse$^{+/+}$ group. The cell number of neutrophils showed no difference in all groups (fig. 5a). As shown in figure 5b, there was a significant increase in *P. pratense*-specific IgG and IgE in plasma after administration of *P. pratense* extract over 11 weeks. This reflects the sensitization to *P. pratense*; however, there was no difference between Ctse$^{+/+}$ and Ctse$^{-/-}$ mice, neither in IgG nor in IgE. As is known from other chronic models, cytokines returned to normal levels (table 2). Figure 5c shows lung cryosections stained according to Azan novum. Sensitized animals showed an increase in cell infiltration (red cell plasma),

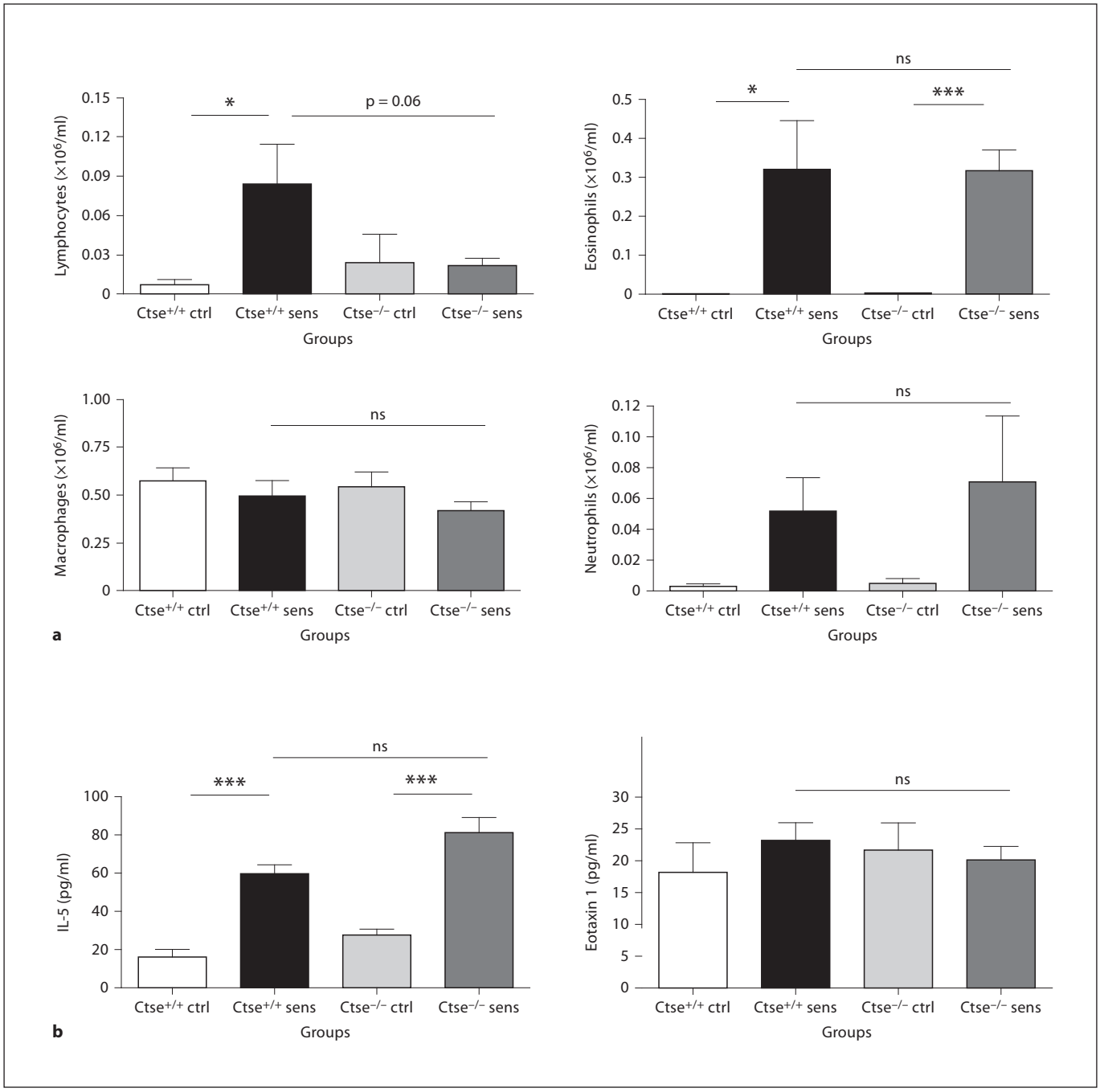
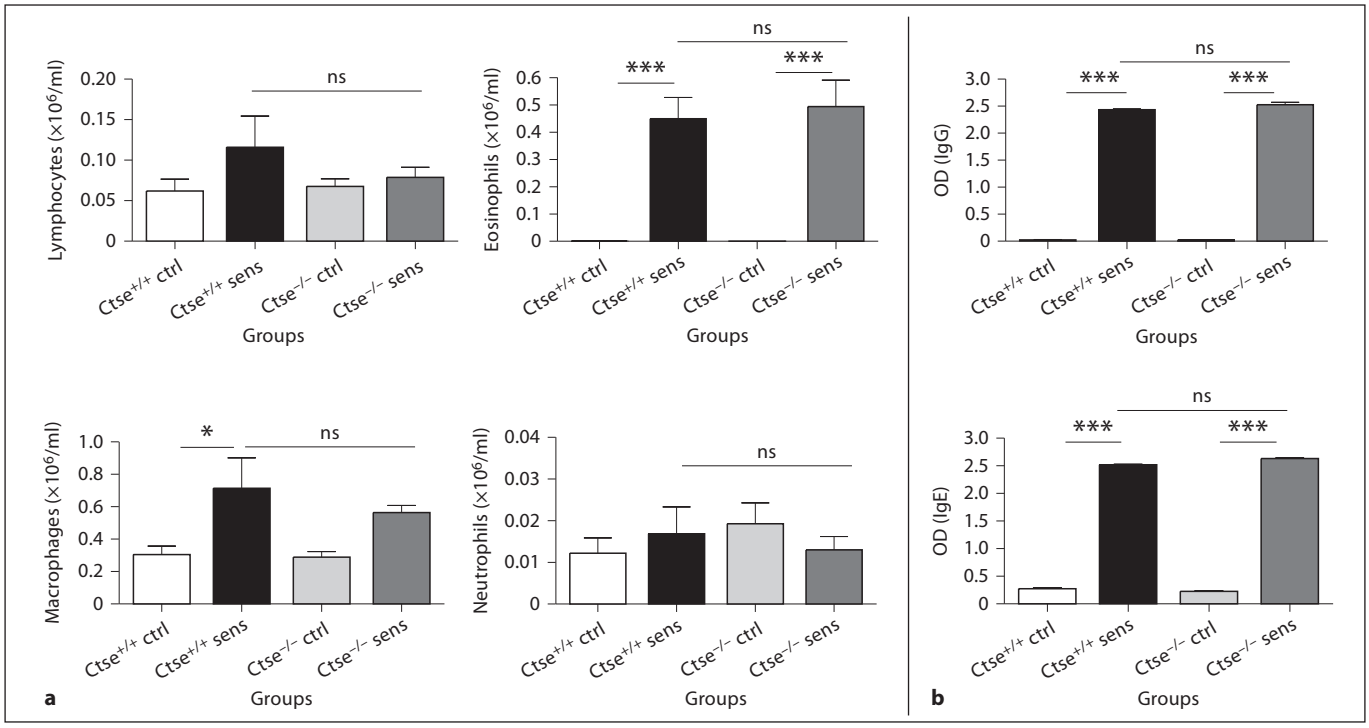


Fig. 4. Ctse$^{-/-}$ deficiency leads to reduced lymphocyte influx after OVA sensitization and challenge. Ctse$^{+/+}$ and Ctse$^{-/-}$ mice were sensitized intraperitoneally with OVA (Ctse$^{+/+}$ sens, Ctse$^{-/-}$ sens). Animals in the control group received saline (Ctse$^{+/+}$ ctrl, Ctse$^{-/-}$ ctrl). **a** BAL differential cell count shows the concentration of lymphocytes, eosinophils, Mph and neutrophils. **b** Cytokine/chemokine levels in pg/ml in BAL were measured in duplicates using ELISA. Bars represent mean ± SEM of n = 7 (Ctse$^{+/+}$ ctrl) or n = 8 (Ctse$^{+/+}$ sens, Ctse$^{-/-}$ ctrl, Ctse$^{-/-}$ sens). * $p < 0.05$ in the t test. ns = Nonsignificant.



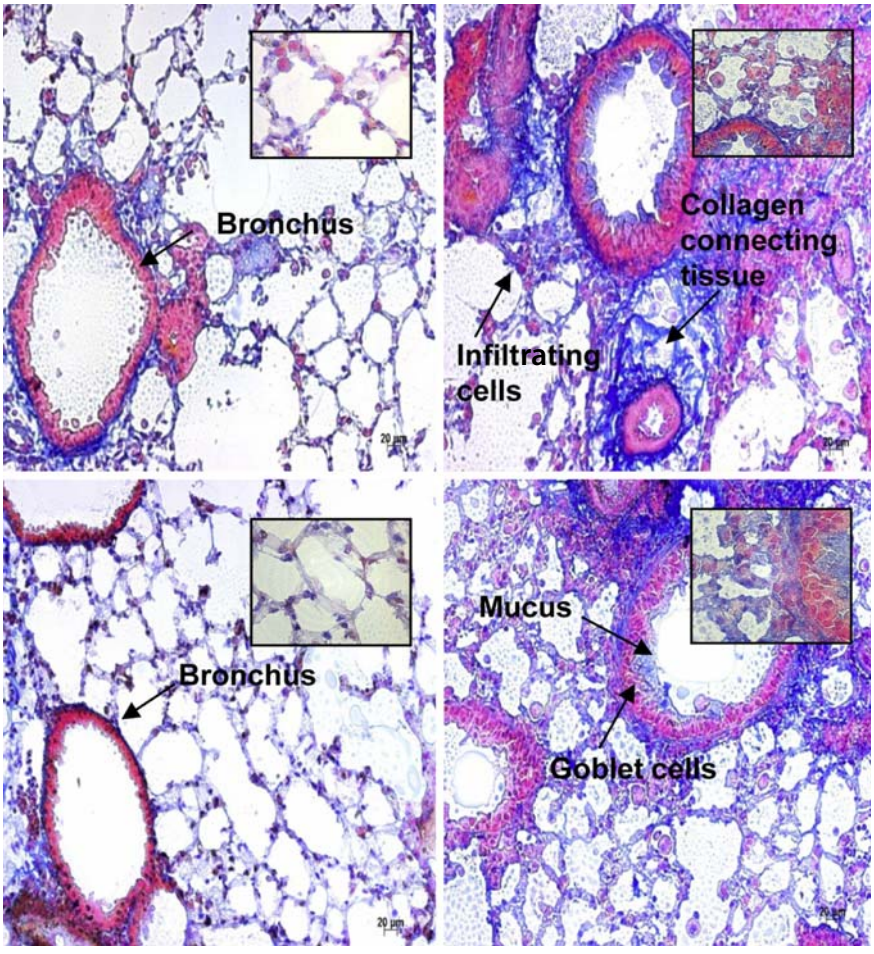


Fig. 5. Reduced lymphocyte infiltration in Ctse$^{-/-}$ mice after *P. pratense* sensitization. Ctse$^{+/+}$ and Ctse$^{-/-}$ mice were sensitized with *P. pratense* extract (Ctse$^{+/+}$ sens, Ctse$^{-/-}$ sens) over a period of 11 weeks. Control mice received NaCl (Ctse$^{+/+}$ ctrl, Ctse$^{-/-}$ ctrl). **a** BAL differential cell count. **b** *P. pratense*-specific IgG and IgE in plasma. **c** Histology of lung cryosections after Azan novum staining showed cell infiltration (red nuclei of the cells), mucus covering the epithelium (blue), goblet cells (red) and collagen connecting tissue (blue) in both sensitized groups. Magnification ×20; inset ×100. Bars represent mean ± SEM of n = 12 (Ctse$^{+/+}$ ctrl, Ctse$^{-/-}$ ctrl, Ctse$^{-/-}$ sens) or n = 6 (Ctse$^{+/+}$ sens). * $p < 0.05$ by one-way ANOVA with Bonferroni correction. ns = Nonsignificant.

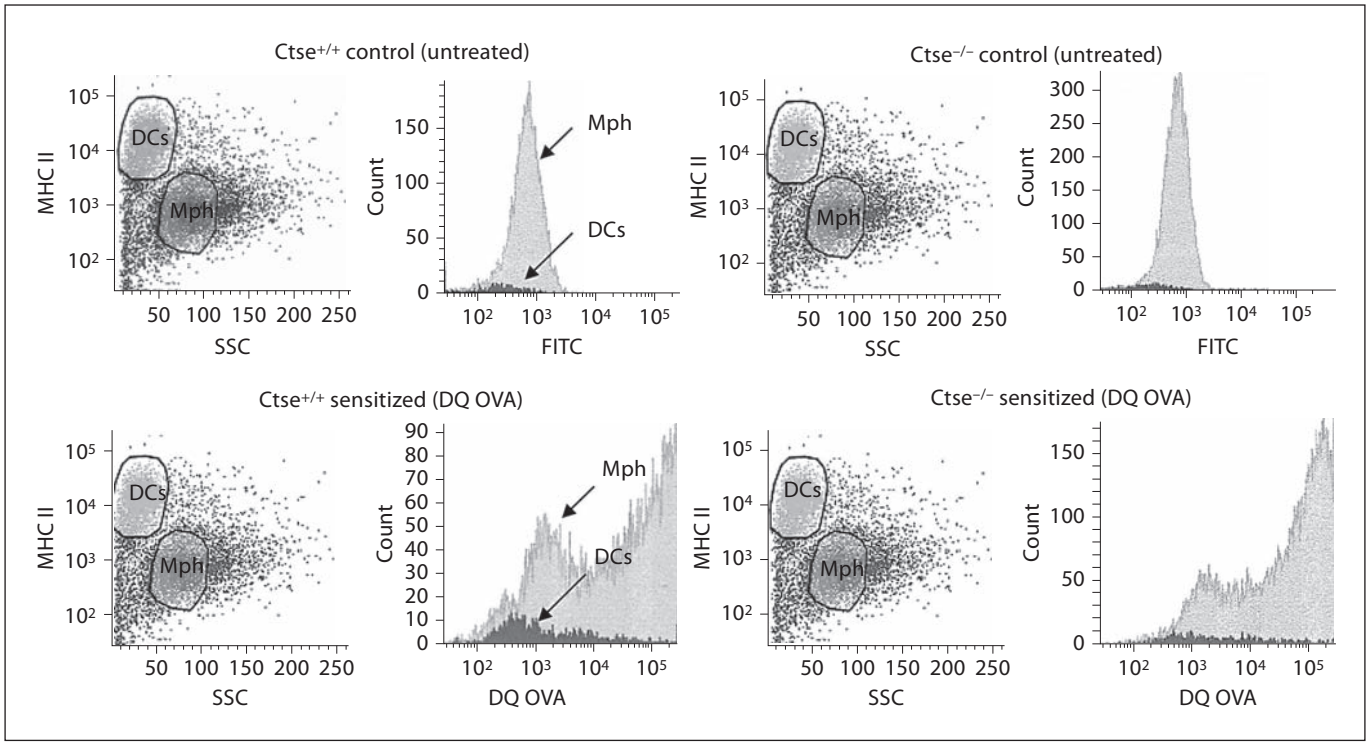


Fig. 6. No difference between lung DCs and Mph of Ctse$^{+/+}$ and Ctse$^{-/-}$ mice in DQ™ ovalbumin processing. Ctse$^{+/+}$ and Ctse$^{-/-}$ mice received 50 μg DQ™ OVA and 0.1 μg LPS (Ctse$^{+/+}$ sens, Ctse$^{-/-}$ sens). Control groups were untreated (Ctse$^{+/+}$ ctrl, Ctse$^{-/-}$ ctrl). Upper panels show MHC II expression and autofluorescence of both control groups, lower panels show MHC II expression and the processed DQ™ OVA of both sensitized groups (DQ™ + LPS) for Mph (light grey) and DC (dark grey) of Ctse$^{+/+}$ and Ctse$^{-/-}$ mice. n = 2.

Table 3. Mean fluorescence intensity of processed DQ^{TM} OVA in lung DCs and lung Mph from Ctse$^{+/+}$ and Ctse$^{-/-}$ mice

Group	Ctse$^{+/+}$ DCs	Ctse$^{+/+}$ Mph	Ctse$^{-/-}$ DCs	Ctse$^{-/-}$ Mph
Control	338	746	334	819
Sensitized	14,497	70,725	19,326	88,239

Ctse$^{+/+}$ and Ctse$^{-/-}$ mice received DQ^{TM} OVA and LPS (sensitized). Control mice were untreated. DCs were identified and sorted as CD11c^{+} MHC II^{high} cells, whereas tissue Mph were separated by MHC-II^{low} phenotype and were analyzed for DQ^{TM} OVA processing. n = 1 (Ctse$^{+/+}$ ctrl, Ctse$^{-/-}$ ctrl), n = 2 (Ctse$^{+/+}$ sens, Ctse$^{-/-}$ sens).

mucus covering the epithelium (blue), goblet cells (red) and collagen connecting tissue (blue) compared to control mice. The sensitized groups thus showed clear signs of remodeling processes. But again, in terms of histological staining, there was also no difference between Ctse$^{+/+}$ and Ctse$^{-/-}$ mice.

No Difference between Lung DCs and Mph of Ctse$^{+/+}$ and Ctse$^{-/-}$ Mice in the Processing of DQ^{TM} OVA

To study mechanisms of antigen processing in Ctse$^{+/+}$ and Ctse$^{-/-}$ mice, DQ™ OVA was used. DQ™ OVA is a self-quenched conjugate of OVA that exhibits bright green fluorescence upon proteolytic degradation.

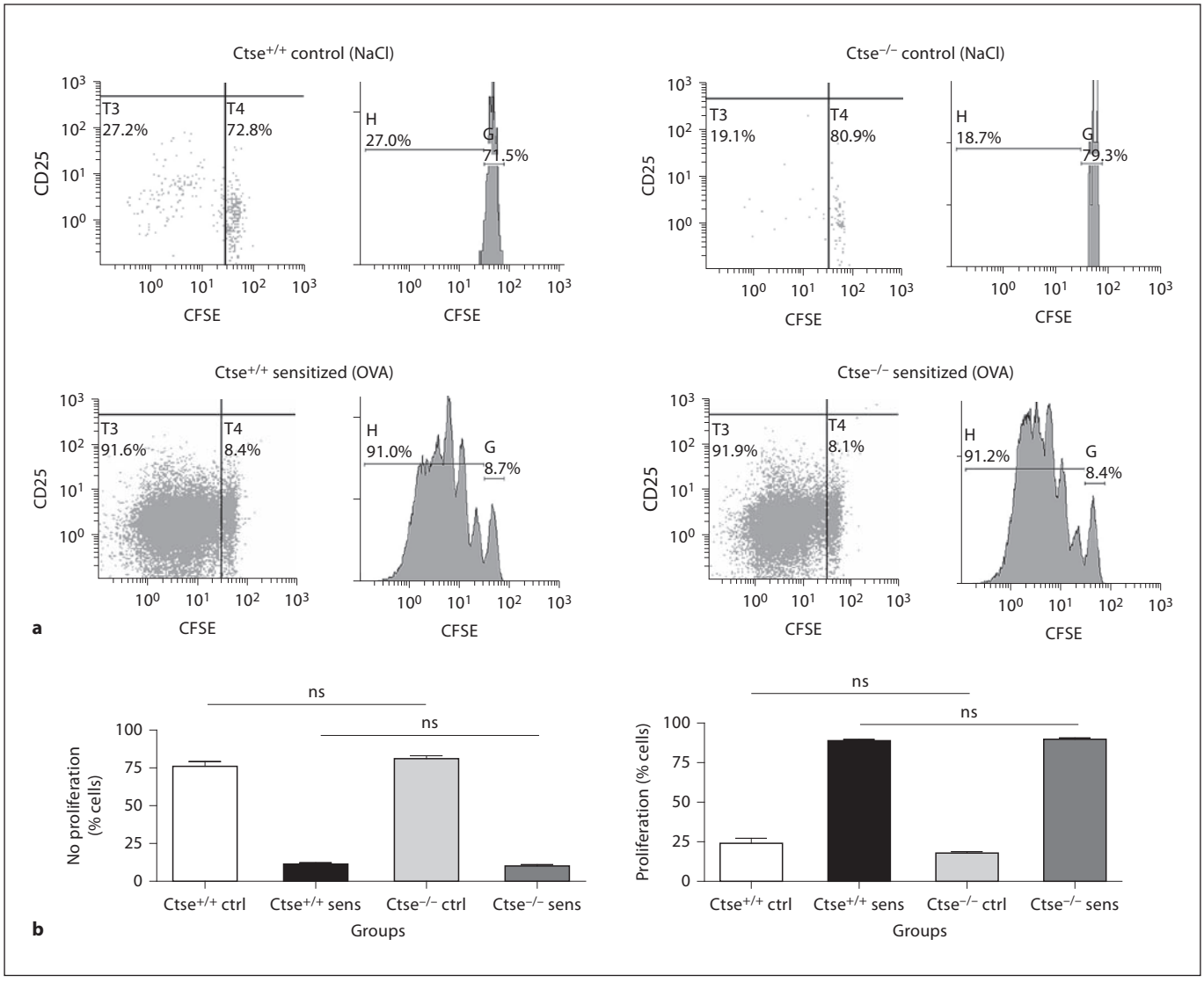


Fig. 7. No difference in proliferation of injected OT II cells in lung-draining lymph nodes of Ctse$^{+/+}$ and Ctse$^{-/-}$ mice. **a** CFSE-labeled OT II cells were injected intravenously into Ctse$^{+/+}$ and Ctse$^{-/-}$ mice. Animals were challenged with OVA aerosol (sensitized). Control mice received saline aerosol. Four days later, lung-draining lymph nodes of Ctse$^{+/+}$ and Ctse$^{-/-}$ mice were isolated and the CFSE proliferation profile for the OT II cells (CD4^{+}, Ly5.1^{+}) was assessed. OT II cells were stained for different cell surface markers such as CD25. Upper panels show the proliferation profile of both control groups (NaCl), lower panels show the proliferation profile of OVA-sensitized Ctse$^{+/+}$ and Ctse$^{-/-}$ mice. **b** The left figure shows the percentage of non-proliferated OT II cells in both control and sensitized groups and the right figure shows the percentage of proliferated OT II cells for both control and sensitized groups. Bars represent mean ± SEM of n = 2 (Ctse$^{+/+}$ ctrl, Ctse$^{-/-}$ ctrl) or n = 6 (Ctse$^{+/+}$ sens, Ctse$^{-/-}$ sens). * $p < 0.05$ by t test; ns = nonsignificant.

Ctse$^{+/+}$ and Ctse$^{-/-}$ mice received intranasally DQ™ OVA combined with LPS on 3 consecutive days. Control mice were untreated. Dendritic cells were identified as CD11c^{+} MHC II^{high} cells, whereas tissue Mph were separated by MHC II^{low} phenotype. As shown in figure 6 and table 3, there was no difference between Ctse$^{+/+}$ and Ctse$^{-/-}$ mice in the processing of DQ™ OVA, neither regarding Mph nor DCs. Mph of both control groups showed higher mean fluorescence intensity compared to DCs of both negative groups because of their autofluorescence.

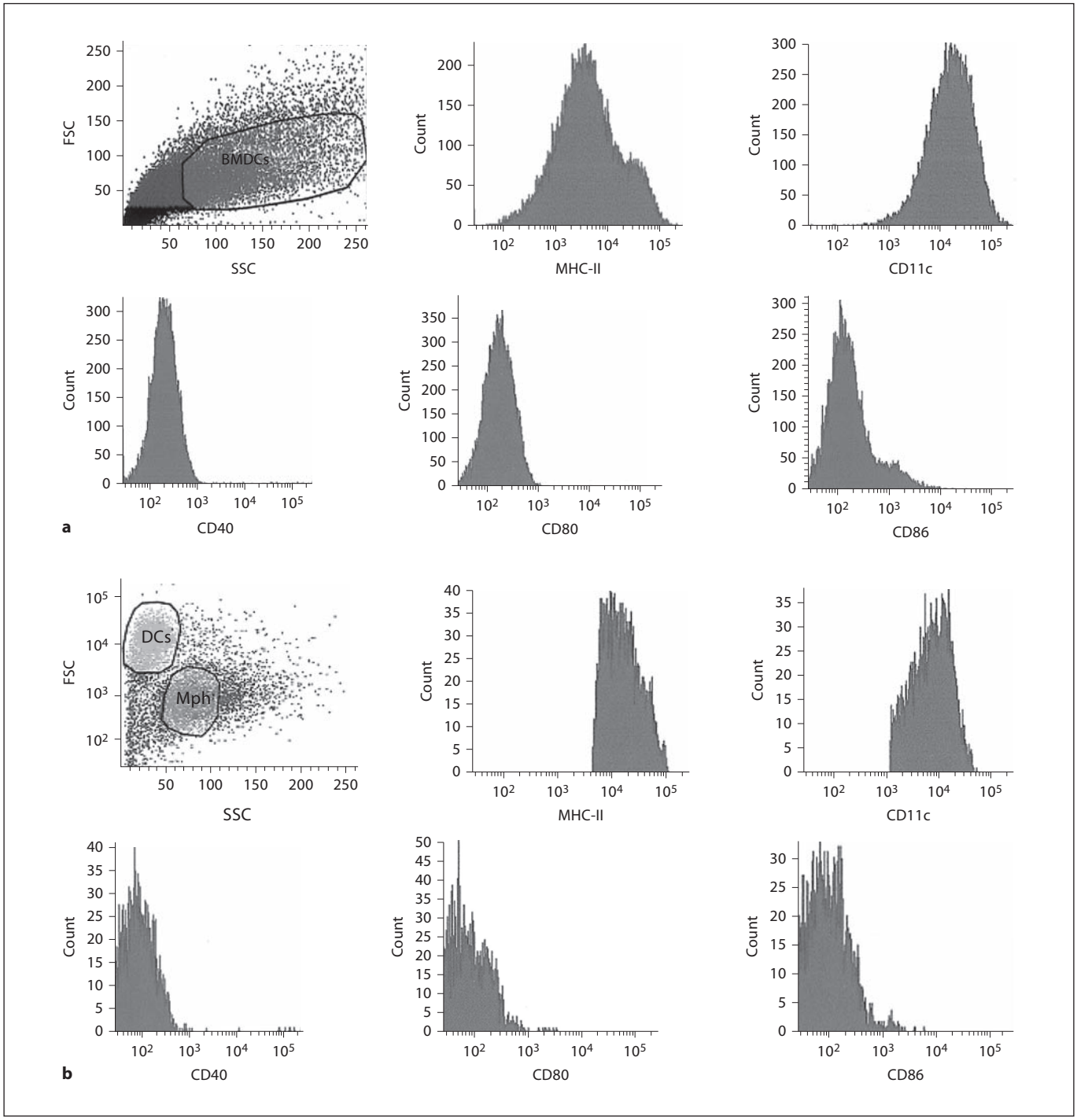


Fig. 8. Expression of cell surface markers on BMDCs and lung DCs. In vitro-generated BMDCs and isolated lung DCs of C57BL/6 mice were stained for different cell surface markers such as PE-labeled MHC II, APC-labeled CD11c, FITC-labeled CD40, CD80 and CD86, or the appropriate isotype controls and were analyzed by flow cytometry. DCs were identified and defined as $CD11c^{+}$ MHC II^{high} cells, whereas tissue Mph were defined as MHC II^{low} phenotype. **a** Dot plot and histograms of the cell surface markers MHC II, CD11c, CD40, CD80 and CD86 on BMDCs. **b** Dot plot and histogram of the cell surface markers MHC II, CD11c, CD40, CD80 and CD86 on lung DCs. Dot plots and histograms show representative results of three independent experiments.

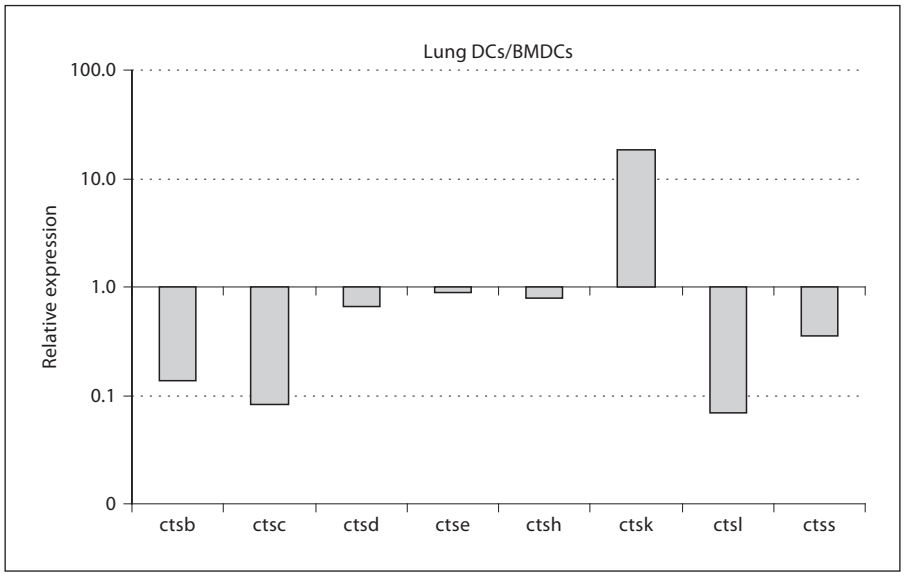


Fig. 9. Ratio of expression of the analyzed cathepsins in lung DCs versus BMDCs. Ratio of expression of cathepsins B, C, D, E, H, K, L and S by real-time PCR in cDNA of in vitro-generated isolated lung DCs versus BMDCs.

Table 4. Concentration, number of transcripts and ratio of the cathepsins B, C, D, E, H, K, L and S in BMDCs and lung DCs normalized to the housekeeping gene PBGD

	BMDCs		Lung DCs		Ratio
	concentration g/l	transcripts mol/l	concentration g/l	transcripts mol/l	
Cathepsin B	4.22×10^{-8}	9.13×10^{9}	1.33×10^{-9}	2.87×10^{8}	0.136
Cathepsin C	9.18×10^{-9}	1.58×10^{9}	1.75×10^{-10}	3.77×10^{7}	0.082
Cathepsin D	9.51×10^{-9}	2.10×10^{9}	1.47×10^{-9}	3.24×10^{8}	0.668
Cathepsin E	6.35×10^{-12}	1.44×10^{6}	1.31×10^{-12}	2.98×10^{5}	0.894
Cathepsin H	1.37×10^{-9}	3.00×10^{8}	2.50×10^{-10}	5.47×10^{7}	0.783
Cathepsin K	1.75×10^{-11}	3.92×10^{6}	7.49×10^{-11}	1.68×10^{7}	18.561
Cathepsin L	6.64×10^{-8}	1.46×10^{8}	1.04×10^{-11}	2.29×10^{6}	0.068
Cathepsin S	3.63×10^{-8}	7.82×10^{9}	2.96×10^{-9}	6.37×10^{8}	0.352

From in vitro-generated BMDCs and isolated lung DCs of naive C57BL/6 mice, RNA was extracted, reverse-transcribed with Omniscript or Sensiscript and cDNA was analyzed for expression of cathepsins B, C, D, E, H, K, L and S by real-time PCR and were normalized to the housekeeping gene PBGD. The concentration, the number of transcripts and the ratio of the cathepsins B, C, D, E, H, K, L and S in lung DCs to BMDCs were analyzed.

No Difference in Proliferation of Injected OT II Cells in Lung-Draining Lymph Nodes of Ctse$^{+/+}$ and Ctse$^{-/-}$ Mice

To find out whether Ctse deficiency has an effect on antigen presentation in vivo, we intravenously injected Ctse$^{+/+}$ and Ctse$^{-/-}$ mice with CFSE-labeled OT II cells. After exposure to OVA or NaCl aerosol, the lung-draining lymph nodes of the Ctse$^{+/+}$ and Ctse$^{-/-}$ mice were isolated 4 days later and the CFSE proliferation profile for the OT II cells (CD4^{+}, Ly5.1^{+}) was assessed by flow cytometry. There was no difference in proliferation of injected OT cells between sensitized Ctse$^{+/+}$ and Ctse$^{-/-}$ mice (fig. 7a, b).

Expression of Cell Surface Markers on BMDCs and Lung DCs

In vitro generated BMDCs and isolated lung DCs were stained for different cell surface markers such as PE-la-

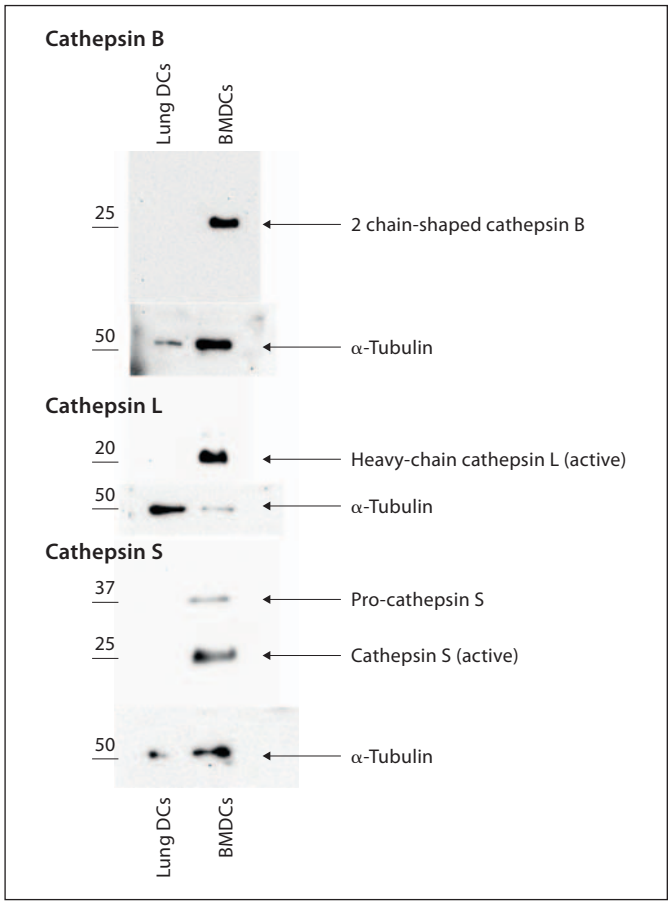


Fig. 10. Western blot analysis of cathepsins B, L and S in isolated lung DCs and in vitro-generated BMDCs. DCs from lung and bone marrow were disrupted and homogenized in lysis buffer. Fifty micrograms of protein from the postnuclear supernatant were resolved by 15% SDS-PAGE and transferred onto PVDF membranes. Cathepsins were detected by the primary antibodies anti-cathepsin B, S and L and the secondary antibody anti-HRP. As a control, α-tubulin was used. Detection of the peroxidase-labeled secondary antibodies was performed by enhanced chemiluminescence reaction (and visualization using the Lumi-Imager system and Lumi-Analyst software).

beled MHC II, APC-labeled CD11c, FITC-labeled CD40, CD80 and CD86 or the appropriate isotype controls, and were analyzed by flow cytometry. As shown in figure 8a, BMDC expressed MHC II, CD11c and CD86 on their cell surface and were negative for CD40 and CD80.

Isolated lung DCs were identified and defined as $CD11c^{+}$MHC II^{high} cells, whereas contaminating tissue Mph were separated by MHC II^{low} phenotype. As shown in figure 8b, lung DCs were $CD11c^{+}$, showed high MHC II expression compared to tissue Mph, and were negative for CD40, CD80 and CD86 after isolation.

Real-Time PCR Analysis of in vitro-Generated BMDCs and Isolated Lung DCs

From in vitro-generated BMDCs and isolated lung DCs of naive C57BL/6 mice, RNA was extracted and reverse-transcribed with Omniscript or Sensiscript, and cDNA was analyzed for the expression of cathepsin B, C, D, E, H, K, L and S, and the housekeeping gene PBGD by real-time PCR. Table 4 shows the concentration, the number of transcripts and the ratio of the cathepsins B, C, D, E, H, K, L and S in lung DCs to those in BMDCs.

Cathepsins B, S, D and C were expressed most and cathepsin L and E were expressed least in in vitro-generated BMDCs. In isolated lung DCs, cathepsins S, D and B were expressed most and cathepsins L and E were expressed least. Figure 9 shows the ratio of expression of the different cathepsins in lung DCs and BMDCs. Cathepsins B, C and L were expressed 10 times less in lung DCs compared to BMDCs, cathepsin S was expressed three times less in lung DCs, and cathepsin K was expressed 20 times more in lung DCs compared to BMDCs. Cathepsins D, E and H showed no difference in expression in lung DCs compared to BMDCs. PCR products were verified via melting curves (fig. 1a) and gel electrophoresis (fig. 1b).

Western Blot Analysis of Cathepsins B, L and S in in vitro-Generated BMDCs and Isolated Lung DCs

Isolated lung DCs and in vitro-generated BMDCs were disrupted in lysis buffer. Fifty micrograms of protein from the postnuclear supernatant were resolved by 15% SDS-PAGE and transferred onto PVDF membranes. Cathepsins were detected by the primary antibodies anti-cathepsin B, S and L and the secondary antibody anti-HRP. α-Tubulin was used as a control. Detection of the peroxidase-labeled secondary antibodies was done by enhanced chemiluminescence reaction (and visualization using the Lumi-Imager system and Lumi-Analyst software). As expected, the proteins of cathepsins B, L and S were found at lower quantities in isolated lung DCs than in in vitro-generated BMDCs (fig. 10).

Discussion

Kakehashi et al. [36] were able to show that Ctse deficiency leads to enhanced OT cell activation in BMDCs due to increased expression of CD80, CD86 and CD40 compared to $Ctse^{+/+}$ mice in vitro. They saw a reduction in OT cell activation in bone marrow-derived Mph because of decreased expression of costimulatory molecules. In contrast, we found a reduction in OT II cell pro-

liferation primed by BMDCs of Ctse$^{-/-}$ mice. In our in vitro study, OT II cells incubated with BMDCs of Ctse$^{-/-}$ mice showed significantly diminished proliferation compared to OT II cells cocultured with BMDCs of Ctse$^{+/+}$ mice. Incubation of OT II cells with bone marrow-derived Mph showed no difference between Ctse$^{-/-}$ and Ctse$^{+/+}$ mice (unpubl. data). Other in vitro studies were also able to show a reduction in proliferation of murine B cells and BMDCs by blocking Ctse with inhibitors. They demonstrated that Ctse plays an important role in the class II MHC antigen processing and presentation pathway [3, 14]. An explanation for these discrepancies was maybe shown by Yee et al. [37]. They found that Ctse expression is negatively regulated by the MHC class II transactivator (CIITA). This is a non-DNA-binding transcription factor which activates and is required for the expression of MHC II and other genes related to antigen presentation. This regulation of Ctse by CIITA might either inhibit or promote antigen processing and presentation [2, 37, 38].

The evidence that the absence of Ctse leads to a reduced antigen presentation in vitro could offer new therapeutic opportunities in allergic diseases such as allergic asthma. In allergic asthma, the processing and presentation of exogenous antigens or allergens is an essential mechanism in the sensitization to an allergen. This allergen can activate DCs to break the process of tolerance and promote the Th2 response in allergic asthma [24]. As mentioned above, Ctse participates in antigen processing and presentation, and therefore plays a role in the sensitization phase of allergic asthma. Ctse deficiency could lead to a decrease in allergen processing and presentation and thus to a decrease in allergic airway inflammation.

Therefore, acute OVA-induced and subchronic *P. pratense*-induced airway inflammation, as established in our lab [35], were investigated in Ctse$^{+/+}$ and Ctse$^{-/-}$ mice. These two airway inflammation models showed a reduced infiltration of lymphocytes in Ctse$^{-/-}$ mice, whereas in the sensitized Ctse$^{+/+}$ group lymphocyte numbers were increased. These results supported the findings from the in vitro experiment. There was no difference, however, between Ctse$^{+/+}$ and Ctse$^{-/-}$ mice in eosinophilic infiltration, Mph numbers and in neutrophilic infiltration in both investigated types of airway inflammation, although Ctse deficiency has been reported to impair chemotaxis and cell adhesion in Mph due to a decrease in several cell-surface receptors such as CCR2 and CD18 or CD29 [39]. The acute model of airway sensitization exhibited a significant increase in IL-5, showing the infiltration of eosinophils, but there was also no difference between sensitized Ctse$^{+/+}$ and Ctse$^{-/-}$ mice. In both investigated airway inflammations models, other cytokines such as IL-4, IL-13 and the chemokine eotaxin showed low levels and no difference between all groups, because these cytokines and the chemokine were secreted in the induction phase of inflammation and returned to normal levels [40]. The airway sensitization in the subchronic protocol resulted in a significant increase in *P. pratense*-specific IgG and IgE in the plasma of sensitized mice, which monitors sensitization to grass pollen allergen in mice, as previously shown [41]. Ongoing inflammation results in structural remodeling, including airway wall thickening, subepithelial fibrosis, and goblet cell hyperplasia, collectively known as airway remodeling [40]. These structural changes could be seen in sensitized Ctse$^{+/+}$ and Ctse$^{-/-}$ mice of the subchronic model. Sensitized Ctse$^{+/+}$ and Ctse$^{-/-}$ mice showed an increase in cell infiltration, mucus covering the epithelium, goblet cells and collagen connective tissue compared to both control groups. Sensitized animals exhibited clear signs of remodeling processes, but again, in terms of histological staining there was no difference between Ctse$^{+/+}$ and Ctse$^{-/-}$ mice.

To investigate the mechanism of antigen processing and presentation in Ctse$^{+/+}$ and Ctse$^{-/-}$ mice in the lung, experiments with DQ™ OVA and with OT II cells were performed. We used DQ™ to examine the mechanism of antigen processing in Ctse$^{+/+}$ and Ctse$^{-/-}$ mice. There was no difference between Ctse$^{+/+}$ and Ctse$^{-/-}$ mice in the processing of DQ™ OVA, neither with regard to Mph nor DC, although Ctse was reported to be involved in OVA processing [41].

In the in vivo study with OT II cells mice which were challenged with OVA aerosol showed a significant increase in proliferation of the injected OT II cells compared to the controls, indicating that the proliferation of OT II cells is antigen-specific. However, there was no difference in proliferation between Ctse$^{+/+}$ and Ctse$^{-/-}$ mice, although Ctse has been reported to play a role in antigen presentation in vitro [3].

Ctse$^{-/-}$ mice showed no T lymphocyte infiltrations in the sensitized groups of induced airway inflammation, but behaved similarly to Ctse$^{+/+}$ mice with regard to eosinophilic recruitment. Ctse deficiency led to no alteration in antigen processing and presentation in vivo. An explanation for this may be based on the redundancy of the inflammatory cascade. In this respect, compensatory effects may be provided by other proteases present in the lung. Real-time PCR analysis of the expression of different cysteine and aspartic cathepsins in isolated lung DCs

of naive C57/BL6 mice showed a lower content of Ctse transcripts (2.98×10^5 mol/l), compared to transcripts of cathepsins S, D and B (6.37×10^8 mol/l, 3.24×10^8 mol/l, 2.87×10^8 mol/l). It was also reported that there was a natural Ctse deficiency in the immune system of C57/BL6 mice [42]. Our real-time PCR results support these findings.

Cathepsin S is the best characterized cathepsin, expressed predominantly in APC, namely DC and B cells [43]. Evidence for its crucial role in antigen processing and presentation was found in cathepsin S-deficient mice. In these mice, APC failed to express MHC class II peptide complexes on their surfaces and therefore they poorly induced T cell proliferation [44].

The aspartic protease cathepsin D is reported to be involved in antigen processing and presentation [45, 46]. The cysteine protease cathepsin B was shown to be elevated in murine lung DCs after infection with influenza A virus leading to enhanced processing and presentation of other antigens such as allergens [47]. In a study with blocking of cathepsins D and B, cathepsin B was found to play an important role in antigen processing, while cathepsin D is involved in degradation of the invariant chain in ovalbumin-immunized mice [48]. Thus other cathepsins such as cathepsins S, D and B are higher expressed in lung DCs and therefore countervail the lack of Ctse in vivo.

Summarizing the present data, Ctse deficiency has an effect on the antigen processing and presentation in vitro. Investigating this effect in an acute airway inflammation model, lymphocyte infiltration in $Ctse^{-/-}$ mice was inhibited without affecting infiltration by other inflammatory cells. Therefore, a distinct role of Ctse in states of allergic airway inflammation can be assumed.

Acknowledgements

The authors would like to thank ALK Abelló for providing the grass pollen extract.

This work was funded by DFG in the Research Training Group 1441/1 'Allergic response in lung and skin' and the SFB 587/B13. The funders had no role in study design, data collection and analysis, decision to publish or preparation of the manuscript.

References

1 Kageyama T, Takahashi K: A cathepsin D-like acid proteinase from human gastric mucosa: purification and characterization. J Biochem 1980;87:725–735.
2 Zaidi N, Kalbacher H: Cathepsin E: a mini review. Biochem Biophys Res Commun 2008;367:517–522.
3 Chain BM, Free P, Medd P, Swetman C, Tabor AB, Terrazzini N: The expression and function of cathepsin E in dendritic cells. J Immunol 2005;174:1791–1800.
4 Zaidi N, Hermann C, Herrmann T, Kalbacher H: Emerging functional roles of cathepsin E. Biochem Biophys Res Commun 2008;377:327–330.
5 Sastradipura DF, Nakanishi H, Tsukuba T, Nishishita K, Sakai H, Kato Y, Gotow T, Uchiyama Y, Yamamoto K: Identification of cellular compartments involved in processing of cathepsin E in primary cultures of rat microglia. J Neurochem 1998;70:2045–2056.
6 Solcia E, Paulli M, Silini E, Fiocca R, Finzi G, Kindl S, Boveri E, Bosi F, Cornaggia M, Capella C: Cathepsin E in antigen-presenting Langerhans and interdigitating reticulum cells: its possible role in antigen processing. Eur J Histochem 1993;37:19–26.
7 Saftig P, Hetman M, Schmahl W, Weber K, Heine L, Mossmann H, Koster A, Hess B, Evers M, von Figura K: Mice deficient for the lysosomal proteinase cathepsin D exhibit progressive atrophy of the intestinal mucosa and profound destruction of lymphoid cells. EMBO J 1995;14:3599–3608.
8 Yoshimine Y, Tsukuba T, Isobe R, Sumi M, Akamine A, Maeda K, Yamamoto K: Specific immunocytochemical localization of cathepsin E at the ruffled border membrane of active osteoclasts. Cell Tissue Res 1995;281:85–91.
9 Zaidi N, Herrmann T, Baechle D, Schleicher S, Gogel J, Driessen C, Voelter W, Kalbacher H: A new approach for distinguishing cathepsin E and D activity in antigen-processing organelles. FEBS J 2007;274:3138–3149.
10 Saku T, Sakai H, Shibata Y, Kato Y, Yamamoto K: An immunocytochemical study on distinct intracellular localization of cathepsin E and cathepsin D in human gastric cells and various rat cells. J Biochem 1991;110:956–964.
11 Tsukuba T, Hori H, Azuma T, Takahashi T, Taggart RT, Akamine A, Ezaki M, Nakanishi H, Sakai H, Yamamoto K: Isolation and characterization of recombinant human cathepsin E expressed in Chinese hamster ovary cells. J Biol Chem 1993;268:7276–7282.
12 Tsukuba T, Okamoto K, Okamoto Y, Yanagawa M, Kohmura K, Yasuda Y, Uchi H, Nakahara T, Furue M, Nakayama K, Kadowaki T, Yamamoto K, Nakayama KI: Association of cathepsin E deficiency with development of atopic dermatitis. J Biochem 2003;134:893–902.
13 Tsukuba T, Yamamoto S, Yanagawa M, Okamoto K, Okamoto Y, Nakayama KI, Kadowaki T, Yamamoto K: Cathepsin E-deficient mice show increased susceptibility to bacterial infection associated with the decreased expression of multiple cell surface Toll-like receptors. J Biochem 2006;140:57–66.
14 Bennett K, Levine T, Ellis JS, Peanasky RJ, Samloff IM, Kay J, Chain BM: Antigen processing for presentation by class II major histocompatibility complex requires cleavage by cathepsin E. Eur J Immunol 1992;22:1519–1524.
15 Nishioku T, Hashimoto K, Yamashita K, Liou SY, Kagamiishi Y, Maegawa H, Katsube N, Peters C, von Figura K, Saftig P, Katunuma N, Yamamoto K, Nakanishi H: Involvement of cathepsin E in exogenous antigen processing in primary cultured murine microglia. J Biol Chem 2002;277:4816–4822.
16 Pavli P, Maxwell L, Van de PE, Doe F: Distribution of human colonic dendritic cells and macrophages. Clin Exp Immunol 1996;104:124–132.

17 Sertl K, Takemura T, Tschachler E, Ferrans VJ, Kaliner MA, Shevach EM: Dendritic cells with antigen-presenting capability reside in airway epithelium, lung parenchyma, and visceral pleura. J Exp Med 1986;163:436–451.
18 Upham JW, Stumbles PA: Why are dendritic cells important in allergic diseases of the respiratory tract? Pharmacol Ther 2003;100:75–87.
19 Bryant P, Ploegh H: Class II MHC peptide loading by the professionals. Curr Opin Immunol 2004;16:96–102.
20 Wilson NS, Villadangos JA: Regulation of antigen presentation and cross-presentation in the dendritic cell network: facts, hypothesis, and immunological implications. Adv Immunol 2005;86:241–305.
21 Bryant P, Ploegh H: Class II MHC peptide loading by the professionals. Curr Opin Immunol 2004;16:96–102.
22 Honey K, Rudensky AY: Lysosomal cysteine proteases regulate antigen presentation. Nat Rev Immunol 2003;3:472–482.
23 Moss CX, Villadangos JA, Watts C: Destructive potential of the aspartyl protease cathepsin D in MHC class II-restricted antigen processing. Eur J Immunol 2005;35:3442–3451.
24 Lambrecht BN, Hammad H: Lung dendritic cells: targets for therapy in allergic disease. Chem Immunol Allergy 2008;94:189–200.
25 Masoli M, Fabian D, Holt S, Beasley R: The global burden of asthma: executive summary of the GINA Dissemination Committee report. Allergy 2004;59:469–478.
26 Marks GB, Correll PK, Williamson M: Asthma in Australia 2005. Med J Aust 2005;183:445–446.
27 van Rijt LS, Lambrecht BN: Dendritic cells in asthma: a function beyond sensitization. Clin Exp Allergy 2005;35:1125–1134.
28 Vermaelen KY, Carro-Muino I, Lambrecht BN, Pauwels RA: Specific migratory dendritic cells rapidly transport antigen from the airways to the thoracic lymph nodes. J Exp Med 2001;193:51–60.
29 Lambrecht BN, Salomon B, Klatzmann D, Pauwels RA: Dendritic cells are required for the development of chronic eosinophilic airway inflammation in response to inhaled antigen in sensitized mice. J Immunol 1998;160:4090–4097.
30 Marathias KP, Preffer FI, Pinto C, Kradin RL: Most human pulmonary infiltrating lymphocytes display the surface immune phenotype and functional responses of sensitized T cells. Am J Respir Cell Mol Biol 1991;5:470–476.
31 Medoff BD, Thomas SY, Banerji A, Wain JC, Zhang H, Lilly CM, Ginns LC, Luster AD: Pathogenic T cell recruitment into the airway in human disease. Ann NY Acad Sci 2005;1062:220–241.
32 Medoff BD, Thomas SY, Luster AD: T cell trafficking in allergic asthma: the ins and outs. Annu Rev Immunol 2008;26:205–232.
33 Lutz MB, Kukutsch N, Ogilvie AL, Rossner S, Koch F, Romani N, Schuler G: An advanced culture method for generating large quantities of highly pure dendritic cells from mouse bone marrow. J Immunol Methods 1999;223:77–92.
34 Nassenstein C, Kammertoens T, Veres TZ, Uckert W, Spies E, Fuchs B, Krug N, Braun A: Neuroimmune crosstalk in asthma: dual role of the neurotrophin receptor p75NTR. J Allergy Clin Immunol 2007;120:1089–1096.
35 Fuchs B, Knothe S, Rochlitzer S, Nassimi M, Greweling M, Lauenstein HD, Nassenstein C, Muller M, Ebensen T, Dittrich AM, Krug N, Guzman CA, Braun A: A Toll-like receptor 2/6 agonist reduces allergic airway inflammation in chronic respiratory sensitisation to Timothy grass pollen antigens. Int Arch Allergy Immunol 2010;152:131–139.
36 Kakehashi H, Nishioku T, Tsukuba T, Kadowaki T, Nakamura S, Yamamoto K: Differential regulation of the nature and functions of dendritic cells and macrophages by cathepsin E. J Immunol 2007;179:5728–5737.
37 Yee CS, Yao Y, Li P, Klemsz MJ, Blum JS, Chang CH: Cathepsin E: a novel target for regulation by class II transactivator. J Immunol 2004;172:5528–5534.
38 Chang CH, Hong SC, Hughes CC, Janeway CA Jr, Flavell RA: CIITA activates the expression of MHC class II genes in mouse T cells. Int Immunol 1995;7:1515–1518.
39 Tsukuba T, Yanagawa M, Okamoto K, Okamoto Y, Yasuda Y, Nakayama KI, Kadowaki T, Yamamoto K: Impaired chemotaxis and cell adhesion due to decrease in several cell-surface receptors in cathepsin E-deficient macrophages. J Biochem 2009;145:565–573.
40 Bloemen K, Verstraelen S, Van Den HR, Witters H, Nelissen I, Schoeters G: The allergic cascade: review of the most important molecules in the asthmatic lung. Immunol Lett 2007;113:6–18.
41 Moss CX, Villadangos JA, Watts C: Destructive potential of the aspartyl protease cathepsin D in MHC class II-restricted antigen processing. Eur J Immunol 2005;35:3442–3451.
42 Tulone C, Tsang J, Prokopowicz Z, Grosvenor N, Chain B: Natural cathepsin E deficiency in the immune system of C57BL/6J mice. Immunogenetics 2007;59:927–935.
43 Hsing LC, Rudensky AY: The lysosomal cysteine proteases in MHC class II antigen presentation. Immunol Rev 2005;207:229–241.
44 van Eijk M, van Noorden CJ, de Groot C: Proteinases and their inhibitors in the immune system. Int Rev Cytol 2003;222:197–236.
45 Hewitt EW, Treumann A, Morrice N, Tatnell PJ, Kay J, Watts C: Natural processing sites for human cathepsin E and cathepsin D in tetanus toxin: implications for T cell epitope generation. J Immunol 1997;159:4693–4699.
46 Rhodes JM, Andersen AB: Role of cathepsin D in the degradation of human serum albumin by peritoneal macrophages and veiled cells in antigen presentation. Immunol Lett 1993;37:103–110.
47 Burster T, Giffon T, Dahl ME, Bjorck P, Bogyo M, Weber E, Mahmood K, Lewis DB, Mellins ED: Influenza A virus elevates active cathepsin B in primary murine DC. Int Immunol 2007;19:645–655.
48 Zhang T, Maekawa Y, Hanba J, Dainichi T, Nashed BF, Hisaeda H, Sakai T, Asao T, Himeno K, Good RA, Katunuma N: Lysosomal cathepsin B plays an important role in antigen processing, while cathepsin D is involved in degradation of the invariant chain inovalbumin-immunized mice. Immunology 2000;100:13–20.